A Microfluidic Channel Flow Cell for Electrochemical ESR

Andrew J. Wain and Richard G. Compton*

Physical and Theoretical Chemistry Laboratory, Oxford University, South Parks Road, Oxford, OX1 3QZ, United Kingdom

Rudolph Le Roux, Sinéad Matthews, Kamran Yunus, and Adrian C. Fisher*

Department of Chemical Engineering, University of Cambridge, New Museums Site, Pembroke Street, Cambridge, CB2 3RA, UK

Received: July 31, 2006; In Final Form: October 10, 2006

The design, fabrication, and characterization of microfluidic channel flow devices for in situ simultaneous hydrodynamic electrochemical ESR is reported. The microelectrochemical reactors consist of gold film electrodes situated within rectangular ducts of height 350 μm and widths in the range 500−2000 μm. The small dimensions of the channels result in minimal dielectric loss when centralized within a cylindrical TE011 resonant cavity, leading to a high level of sensitivity. This is demonstrated by using the one-electron oxidation of *N*,*N*,*N*′,*N*′-tetramethyl-*p*-phenylenediamine (TMPD) in acetonitrile as a model system, wherein the ESR spectra obtained for the corresponding stable radical cation are of a high signal-to-noise ratio. Signal intensity is measured as a function of flow rate for this system, and the behavior is validated by means of 3-dimensional numerical modeling of the hydrodynamic flow profile.

Introduction

It is well-established that the measurement of voltammetry under conditions of hydrodynamic flow can greatly simplify electrochemical problems, by allowing the dominant mode of mass transport to be carefully controlled and hence the experimental time scale varied.[1,2] In particular, the channel electrode has received a wealth of attention, which has demonstrated that the consideration of mathematically well-defined convection may permit rigorous treatment of mechanistic features of electrode reactions and facilitate the extraction of a range of kinetic information from experimental data.[3−9] A notable application of the channel electrode is in electron spin resonance spectroscopy (ESR); this spectroelectochemical methodology has been demonstrated to provide significant insights into the identity and reactivity of paramagnetic species.[10] In channel flow cell applications the device is held within the resonant cavity of an ESR spectrometer, and paramagnetic species generated at the electrode surface can be simultaneously characterized and quantified according to the structure and intensity of the ESR spectrum observed.[6−8,11] By modeling the concentration profile of the electrogenerated radical species downstream of the electrode, the ESR signal intensity and its variation with solution flow rate can be predicted for stable and reactive species, and in the latter case, kinetic parameters for homogeneous decay can be deduced.[11]

In the past, channel flow cells employed in ESR spectroelectrochemistry have been of a flat geometry with a high aspect ratio, typically of cross section 6 mm × 0.4 mm,[8] which is optimal for use in a rectangular TE_{102} cavity where a maximum in sensitivity occurs along a centralized plane. Significant dielectric absorption occurs outside of this region, and so in this geometry it is crucial to confine lossy solvents to this central plane. An alternative to the rectangular cavity is a cylindrical TE_{011} cavity, used ideally with small solution volumes, in which the maximum sensitivity and minimum dielectric loss is observed along a central axis. Although this cavity mode is clearly not compatible with the flat cell geometry, it is known to have a notably greater sensitivity than the rectangular form,[12] and so by optimizing cell design to the cylindrical geometry, there is scope for improvement of this in situ technique. One approach has employed tubular flow cells and this has been used successfully in the study of a range of systems,[13−17] though further improvements were envisaged on the basis of reducing cell size and solution volume.

The field of microfluidics has seen rapid development over the past decade, with a great deal of focus in the fabrication of "lab on a chip" devices[18−20] and the numerical simulation of such devices.[21,22] As such, the miniaturization of electrochemical reactors by use of photoetchable materials has become widespread, with the application of photolithographic techniques allowing the deposition of electrode films of well-defined geometry.[19,23−27] These fast emerging microreactor construction methodologies might therefore be used to address the current problem of in situ electrochemical ESR, by allowing the assembly of a channel flow cell in which lossy solution is confined to a narrow and well-defined region, which can be situated to run axially along the center of a cylindrical cavity. In this way, minimizing dielectric losses may greatly improve the sensitivity of the spectroelectrochemical approach, without compromising the hydrodynamic behavior of the flow cell. There are further possible advantages associated with the use of a microelectrochemical reactor for ESR, such as reduced ohnmic distortions and ease of potential control as compared to large scale electrochemical cells,[28] and also the reduction of microwave leakage out of the ESR cavity via electrode connections due to their fine dimensions and precise location inside the cavity.

* Address correspondence to these authors. E-mail: richard.compton@chemistry.oxford.ac.uk and acf42@cam.ac.uk.

10.1021/jp064903b CCC: $33.50
Published on Web 11/30/2006

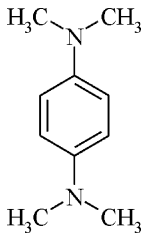

Figure 1. Structure of *N*,*N*,*N*′,*N*′-tetramethyl-*p*-phenylenediamine (TMPD).

In this paper we report the fabrication and characterization of a new generation of electrochemical ESR flow cell with narrow, but well-defined channel dimensions, suitable for use in a cylindrical ESR cavity. The channel cross section of the microelectrochemical reactors does not exceed 0.7 mm^2, thus confining the electrolyte to the sensitive axis of the cavity. Three cells of different channel widths are characterized by use of the one-electron oxidation of *N*,*N*,*N*′,*N*′-tetramethyl-*p*-phenylenediamine (TMPD, see Figure 1) in acetonitrile as a model system. The hydrodynamic voltammetry is shown to be not significantly distorted by ohmic drop, and the steady-state limiting currents are shown to be in agreement with the Levich equation. ESR spectra obtained for the $TMPD^{\bullet+}$ radical cation are of a high signal-to-noise ratio and resolution and the variation of signal intensity with solution flow rate is investigated. Three-dimensional numerical modeling was used to rationalize the signal-flow rate behavior for the three cell geometries. With this theoretical and computational framework in place, the extension of digital simulation to reactive radical systems, such as those pertaining to EC, EC_2, and ECE mechanisms, should be trivial.

Theory

In this section a three-dimensional model of the mass transport and electrolysis reactions occurring within the electrochemical ESR cell is outlined. The cell consists of a rectangular duct and for the purposes of this paper a transport-limited one-electron oxidation of A is simulated

$$A - e_{(m)}^{-} \rightarrow B$$

at the working electrode where sufficient electrolyte has been added to the solution so migratory transport may be neglected. The three-dimensional mass transport equation of interest is then given by

$$D\frac{d^2C}{dx^2} + D\frac{d^2C}{dy^2} + D\frac{d^2C}{dz^2} + u\frac{dC}{dx} + v\frac{dC}{dy} + w\frac{dC}{dz} = 0 \quad (1)$$

where C is the concentration of a species, D is the diffusion coefficient, t is the time, and u, v, and w are the velocities of the solution in the x, y, and z directions, respectively. To calculate the concentration distribution within the cell from (1) it is first necessary to solve the relevant fluid dynamic equations and determine u, v, and w, where p is the pressure, ρ is density, and μ is the viscosity. In this article it is assumed that the fluid is Newtonian and incompressible in behavior so the steady-state Navier Stokes equations are solved[29,30] subject to appropriate boundary conditions by application of numerical methods such as the finite element method,[31] or in restricted cases of laminar flow the 3-dimensional solution velocity can be predicted analytically[32] provided a sufficient lead in length is present to enable the flow to become fully developed[33]

$$v_x = \frac{16\beta^2}{\pi^4}\sum_{n(\mathrm{odd})}^{\infty}\sum_{m(\mathrm{odd})}^{\infty}\frac{\sin\left(n\pi\frac{\xi}{a}\right)\sin\left(m\pi\frac{\eta}{b}\right)}{nm(\beta^2n^2 + m^2)} \quad (2)$$

where a is the cell width, b is the channel height, β is the height: width ratio, ξ is the position along the z-axis, and η is the position along the y-axis. The summation is performed with use of $n = 1, 3, 5, \ldots$ and $m = 1, 3, 5, \ldots$. Numerical simulations were carried out by using a finite difference approach as described previously[34] to permit the calculation of the resultant concentration distribution within the reactor.

Once the steady-state 3D concentration distribution was found, the predicted current measured through the electrode could be calculated numerically

$$i = -nFDAJ \quad (3)$$

where i is the current, n is the number of electrons transferred per reaction, F is the Faraday constant, D is the diffusion coefficient, A is the electrode area, and J is the concentration flux at the surface of the electrode.

Calculations of the ESR signal intensity follow an analogous approach reported previously for 2-dimensional problems where the strength is calculated by convoluting the $\sin^2$ sensitivity of the cavity with the number of spins and integrating the spins throughout the cavity such that:

$$S = S_0\int_{-x_u}^{x_d}\sin^2\left[\frac{(x - x_c)\pi}{l}\right]\left(\int_0^{2h} c(x,y)\,dy\right)dx \quad (4)$$

where S is the signal strength, S_0 is the signal due to one mole of the radical species in the cavity, x_d and x_u are the respective x coordinates upstream and downstream of the cavity, l is the length of the cavity, x_c is the x coordinate at the center of the cavity, and c is the concentration of the radical species in the x and y coordinates calculated through integrating with respect to the width $2h$ of the cavity.

Experimental Section

Cell Fabrication. To obtain the precise cell geometries (Figure 2) a two-stage photolithographic approach was used in the construction of the microelectrochemical reactors. An illustration of the fabrication procedure is outlined in Figure 3.

In the first fabrication stage, a set of gold working and reference electrodes having typical dimensions of 1 and 2 mm respectively are produced via a positive photoresist (Microposit S1828) after subsequent UV exposure to transfer the pattern of the mask to this resist. A layer of titanium and gold is then evaporated onto this substrate, with a total thickness of approximately 200 nm. Removal of the unexposed regions of the resists results in a set of glass embedded gold working and reference electrodes positioned upstream of the edge of the cavity with a counter gold electrode positioned downstream of the edge of the cavity. This was a design requirement to minimize any additional noise artefacts in the spectra due to the interaction of the metal electrodes with the incident microwaves. The second fabrication stage involved the production of a microchannel with a suitable length that traversed both working and counter electrodes and was situated between the inlet and outlet feed tubes to the microreactor. This was achieved by using a negative resist (Microposit SU8) that was spun onto the glass substrate containing the gold electrode pattern (fabricated in the previous stage) to a thickness of 350 μm. Subsequent exposure of this resist to UV light under the desired

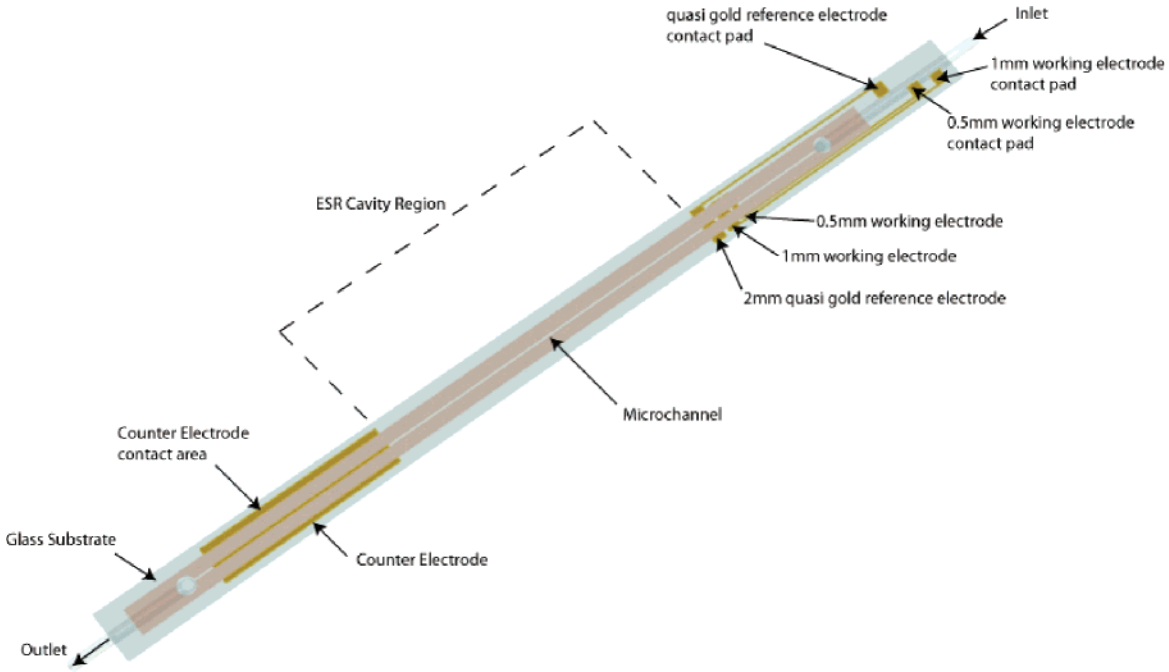

Figure 2. Cell schematic of the microelectrochemical reactor.

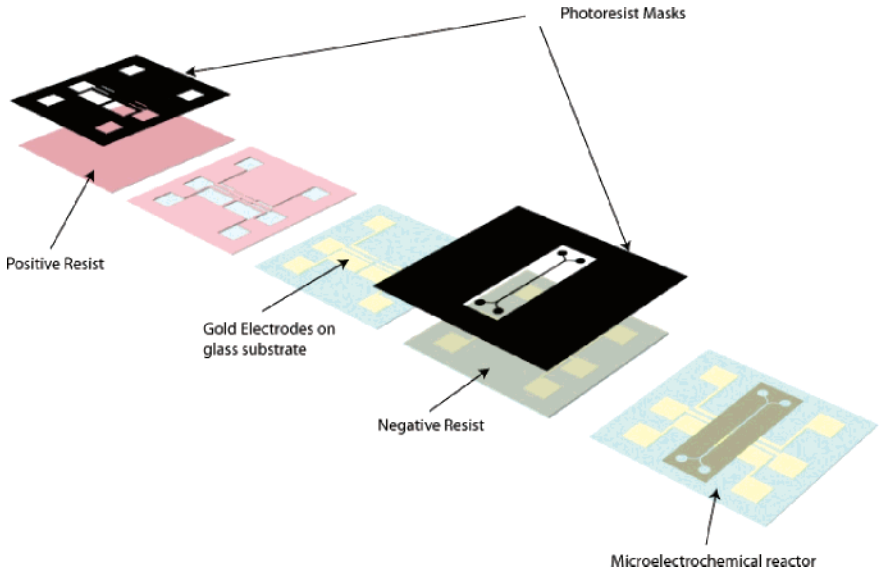

Figure 3. Schematic of the microfabrication procedure for electrochemical ESR cell construction.

microchannel patterned mask yielded a microchannel upon development in a developer solution (Microposit EC developer). Three geometries having a channel width of 0.5, 1.0, and 2.0 mm respectively were fabricated to obtain an optimum channel geometry that would yield quantitative data in both the electrochemical and ESR characterization. Electrical contact was made to the working, reference, and counter electrodes via connection with copper wire (radius 200 μm). Another important design criteria involved the optimal placement of the working electrode from the inlet. This would ensure greater confidence in the assumption of the Lévêque approximation made during the simulated study due to the occurrence of fully developed flow prior to the electrolysis of material.

Chemical Reagents. Electrochemical experiments were carried out in acetonitrile purchased from Fisher with 0.1 M tetra-*N*-butylammonium perchlorate (TBAP, Fluka, puriss. electrochemical grade) as supporting electrolyte. *N*,*N*,*N*′,*N*′-Tetramethylphenylenediamine (TMPD) was purchased from Aldrich. All reagents used were of the highest commercially available grade and were used without further purification. All electrolyte solutions were purged with oxygen-free nitrogen (BOC Gases, Guildford, Surrey, UK) for at least 30 min prior to experimentation.

Apparatus. Potential control was achieved by using a computer-controlled PGSTAT30 potentiostat (Autolab, Eco Chemie, Utrecht, The Netherlands). Fluid motion was maintained with use of a gravity flow system, as used previously, employing glass capillaries to achieve slower flow rates. The volume flow rates employed were in the range 0.2×10^{-3} to 70×10^{-3} cm^3 s^{-1}.

ESR spectra were obtained by using a JEOL JES-FA100 X-band spectrometer with a cylindrical (TE_{011}) cavity resonator. To account for variations in the cavity *Q* factor, signal integrations were measured relative to a standard marker

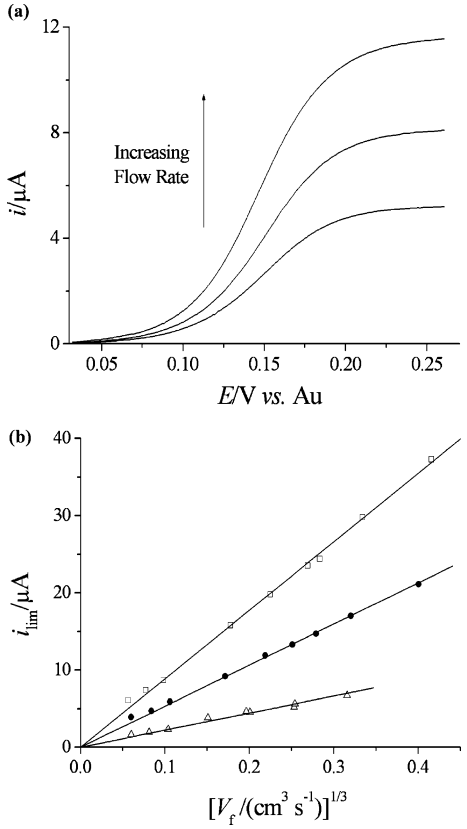

Figure 4. (a) Hydrodynamic voltammetry of 1 mM TMPD in supported acetonitrile, using a 1 mm wide channel flow cell, at flow rates in the range 10^{-3} to 10^{-2} cm^3 s^{-1}. (b) Limiting currents plotted as a function of flow rate for 1 mM TMPD, for three channel widths: 0.5 (△), 1.0 (●), and 2.0 mm (□).

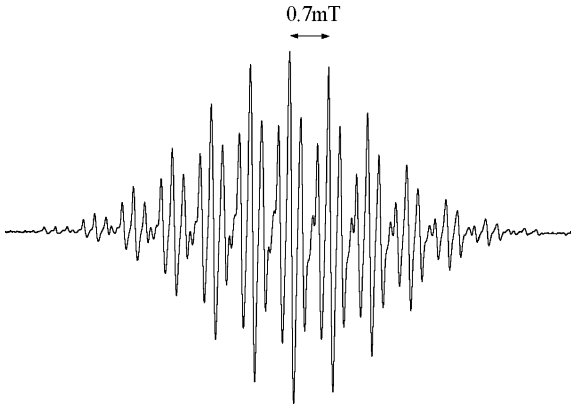

Figure 5. ESR spectrum observed upon electrolysis of TMPD, using a 1 mm wide channel flow cell and an applied potential of +0.25 V (vs pseudo-Au reference electrode), employing a magnetic field modulation width of 0.02 mT.

consisting of solid MgO dispersed with Mn^{2+} inserted into the cavity at the time of measurement. In all ESR experiments, a microwave power of 1 mW was used and regular tests were carried out to confirm that increasing the microwave power increased the ESR signal. Doing so ensured that the system was not power saturated such that the ESR signal intensity gave a direct measure of the number of electrogenerated spins in the cavity. All experiments were conducted at 20 °C.

Results and Discussion

The channel flow cells were characterized by using the single electron oxidation of *N*,*N*,*N*′,*N*′-tetramethyl-*p*-phenylenediamine

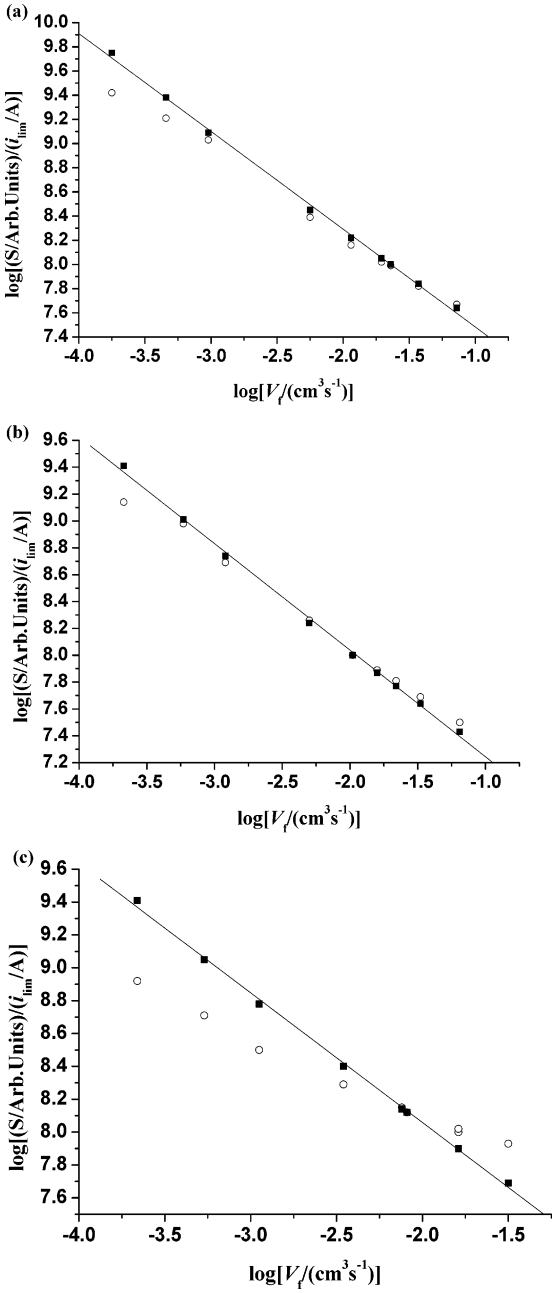

Figure 6. Plots of current normalized ESR signal intensity (S/i_{lim}) as a function of volume flow rate for (a) 2.0 , (b) 1.0, and (c) 0.5 mm wide channel cells: simulation (■) and experiment (○).

(TMPD) in acetonitrile as a model system, since the process is known to be chemically and electrochemically reversible, and the $TMPD^{\bullet+}$ radical cation, "Wurster's Blue", is known to be stable over the timescales employed in this work:[12,15,35,36]

$$TMPD - e^- \rightarrow TMPD^{\bullet+}$$

Flow cells with channel widths of 0.5, 1.0, and 2.0 mm were tested with 1 mM TMPD in acetonitrile containing 0.1 M TBAP, and Figure 4a shows typical hydrodynamic voltammograms for the TMPD oxidation ($E = +0.15$ V vs quasi-Au reference) at a range of flow rates for the 1.0 mm case. The voltammetric waveshape appears undistorted and Tafel plots of E vs $\log(1/i - 1/i_{lim})$, where i is the current measured at the potential, E, and i_{lim} is the mass transport limiting current, were found to be linear in the central electron transport limited region with slopes of 52.2 mV $decade^{-1}$, close to that expected for reversible

electron transfer (58 mV decade^{-1} at 293 K)[37] in the absence of significant Ohmic distortions.[24] Furthermore, the measurement of stable voltammetry would suggest that the gold quasi-reference electrode situated within the channel is acceptable. Plots of limiting current against the cube root of volume flow rate were found to be linear, as shown in Figure 4b, in accordance with the numerical simulations indicating that the cells were behaving quantitatively. It should be noted some deviation for the narrowest cell is observed, which is believed to occur due to the increased resistance of the narrow duct and the significant working electrode to counter electrode path length.

The in situ behavior of each cell was next investigated by centralising them within the cylindrical ESR cavity, with the downstream edge of the working electrode being situated at the upstream edge of the sensitive region of the cavity. Electrolysis of 1 mM TMPD in acetonitrile at the relevant oxidation potential allowed the acquisition of the ESR spectrum shown in Figure 5. The spectrum corresponds to that of the $TMPD^{\bullet+}$ radical cation, and the hyperfine structure is in good agreement with previous reports.[11,14] It is interesting to note that at the slowest volume flow rate, the highest signal-to-noise ratio was observed for the 1 mm channel (S:N $\sim$ 280), suggesting a tradeoff between a greater build up of electrogenerated spins in the wider 2.0 mm channel (S:N $\sim$ 270) and the higher sensitivity due to less dielectric in the narrower 0.5 mm channel (S:N $\sim$ 40).

ESR signal intensity measurements were recorded for each flow cell as a function of flow rate for the TMPD system and the results are plotted in Figure 6 in logarithmic form. In each case the log of the current normalized ESR signal, S/i_{lim}, varies linearly with the log of the volume flow rate and the measured slopes were -0.46, -0.69, and -0.70 for the 0.5, 1.0, and 2.0 mm channels, respectively. The simulated response predicts for a stable electrogenerated radical species this slope should approach $-^2/_3$ under conditions of hydrodynamic flow where the thin diffusion layer (Lévêque) approximation[2] is applicable. This is observed quantitatively for the case of the 1.0 and 2.0 mm width channels, but deviation is noted again from the narrow cell (500 μm) where the current is not entirely consistent with that predicted numerically. This is most likely to arise from the increased resistance associated with the finer channel.

Conclusion

The design development and application of microfabricated microchannels for electrochemical ESR applications have been presented. Quantitative hydrodynamic voltammetry has been performed with simultaneous ESR spectra and signal intensity studies carried out for the one-electron oxidation of TMPD in acetonitrile solution. Numerical simulations which predict the 3-dimensional current and ESR signal intensity have been presented and compared to the experimental response observed. Good agreement between numerical and experimental results has been observed and the ability to extend the numerical simulations to permit more complex mechanistic analysis to be carried out has been noted.

Acknowledgment. A.J.W. thanks the EPSRC and JEOL for funding and S.M. thanks Syngenta Ltd and KY e2v Technologies for funding.

References and Notes

(1) Unwin, P. R.; Compton, R. G. *Compr. Chem. Kinet.* **1989**, 29.

(2) Levich, V. G. *Physicochemical Hydrodynamics*; Prentice Hall: Englewood Cliffs, NJ, 1962.

(3) Cooper, J. A.; Compton, R. G. *Electroanalysis* **1998**, *10*, 141.

(4) Leslie, W. M.; Compton, R. G.; Silk, T. J. *Electroanal. Chem.* **1997**, *424*, 165.

(5) Compton, R. G.; Dryfe, R. A. W. *J. Electroanal. Chem.* **1994**, *375*, 247.

(6) Compton, R. G.; Coles, B. A.; Pikington, M. B. G.; Bethell, D. *J. Chem. Soc., Faraday Trans.* **1990**, *86*, 663.

(7) Compton, R. G.; Dryfe, R. A. W.; Eklund, J. C.; Page, S. D.; Hirst, J.; Nei, L.; Fleet, G. W. J.; Hsia, K. Y.; Bethell, D.; Martingale, L. J. *J. Chem. Soc., Perkin Trans. 2* **1995**, 1673.

(8) Coles, B. A.; Compton, R. G. *J. Electroanal. Chem.* **1983**, *144*, 87.

(9) Compton, R. G.; Pikington, M. B. G.; Stearn, G. M. *J. Chem. Soc., Faraday Trans. 1* **1988**, *84*, 2155.

(10) Bagchi, R. N.; Bond, A. M.; Scholz, F. *Electroanalysis* **1988**, *1*, 1.

(11) Wadhawan, J. D.; Compton, R. G. *Encyclopedia of Electrochemistry*; Bard, A. J., Stratmann, M., Eds.; Wiley-VCH Verlag GmbH and Co. kGaA: Weinheim, Germany, 2003; Vol. 2, Chapter 3.

(12) Weil, J. A.; Bolton, J. R.; Wertz, J. E. *Electron Paramagnetic Resonance, Elementary Theory and Practical Applications*; John Wiley and Sons: New York, 1994.

(13) Streeter, I.; Wain, A. J.; Davis, J.; Compton, R. G. *J. Phys. Chem. B* **2005**, *109*, 18500.

(14) Wain, A. J.; Streeter, I.; Thompson, M.; Fietkau, N.; Drouin, L.; Fairbanks, A. J.; Compton, R. G. *J. Phys. Chem. B* **2006**, *110*, 2681.

(15) Wain, A. J.; Thompson, M.; Klymenko, O. V.; Compton, R. G. *Phys. Chem. Chem. Phys.* **2004**, *6*, 4018.

(16) Wain, A. J.; Compton, R. G. *J. Electroanal. Chem.* **2006**, *587*, 203.

(17) Wain, A. J.; Drouin, L.; Compton, R. G. *J. Electroanal. Chem.* **2006**, *589*, 128.

(18) Tabeling, P. *Introduction to Microfluidics*; Oxford University Press Inc.: New York, 2005.

(19) Ehrfeld, W.; Hessel, V.; Löwe, H. *Microreactors*; Wiley-VCH Verlag GmbH: Weinheim, Germany, 2000.

(20) Jayashree, R. S.; Gancs, L.; Choban, E. R.; Primak, A.; Natarajan, D.; Markoski, L. J.; Kenis, P. J. A. *J. Am. Chem. Soc.* **2005**, *127*, 16759.

(21) Bazylak, A.; Sinton, D.; Djilali, N. *J. Power Sources* **2005**, *143*, 57.

(22) Erickson, D. *Microfluid Nanofluid* **2005**, *1*, 301.

(23) Yunus, K.; Fisher, A. C. *Electroanalysis* **2003**, *15*, 1782.

(24) Yunus, K.; Marks, C. B.; Fisher, A. C.; Allsopp, D. W. E.; Ryan, T. J.; Dryfe, R. A. W.; Hill, S. S.; Roberts, E. P. L.; Brennan, C. M. *Electrochem. Commun.* **2002**, *4*, 579.

(25) Fulian, Q.; Gooch, K. A.; Fisher, A. C.; Stevens, N. P. C.; Compton, R. G. *Anal. Chem.* **2000**, *72*, 3480.

(26) Stevens, N. P. C.; Fulian, Q.; Gooch, K. A.; Fisher, A. C. *J. Phys. Chem. B* **2000**, *104*, 7110.

(27) Wang, J. *Talanta* **2002**, *56*, 223.

(28) Coles, B. A.; Compton, R. G.; Spackman, R. A. *Electroanalysis* **1993**, *5*, 41.

(29) Taylor, C.; Hughes, T. G. Pineride Press., 1981.

(30) Geankoplis, C. J. Allyn and Bacon Inc., 1983.

(31) Henley, I. E.; Fisher, A. C. *J. Phys. Chem. B* **2003**, *107*, 6579.

(32) Spiga, M.; Morini, G. L. *Int. Commun. Heat Mass Transfer* **1994**, *21*, 469.

(33) Henley, I. E.; Fisher, A. C. *Electroanalysis* **2003**, *21*, 55.

(34) Matthews, S. M.; Du, G. Q.; Fisher, A. C. *J. Solid State Electrochem.* **2006**, *10*, 817.

(35) Wang, R. L.; Tam, K. Y.; Compton, R. G. *J. Electroanal. Chem.* **1997**, *434*, 105.

(36) Jacob, S. R.; Hong, Q.; Coles, B. A.; Compton, R. G. *J. Phys. Chem. B* **1999**, *103*, 2963.

(37) Albery, W. J. *Electrode Kinetics*; Clarendon Press: Oxford, 1975.